Telegraph Flux Noise Induced Beating Ramsey Fringe in Transmon Qubits

Zhi-Hao Wu(武志豪)[1], Ling-Xiao Lei(雷凌霄)[2*], Xin-Fang Zhang(张鑫方)[1*], Shi-Chuan Xue(薛诗川)[1], Shun Hu(胡顺)[1], Cong Li(李璁)[1], Xiang Fu(付祥)[1], Ping-Xing Chen(陈平形)[2], Kai Lu(卢凯)[1], Ming-Tang Deng(邓明堂)[1*], and Jun-Jie Wu(吴俊杰)[1]

[1]*College of Computer Science and Technology, National University of Defense Technology, Changsha 410073, China*
[2]*College of Science, National University of Defense Technology, Changsha 410073, China*

(Received 27 February 2025; accepted manuscript online 25 March 2025)

Ramsey oscillations typically exhibit an exponential decay envelope due to environmental noise. However, recent experiments have observed nonmonotonic Ramsey fringes characterized by beating patterns, which deviate from the standard behavior. These beating patterns have primarily been attributed to charge-noise fluctuations. In this paper, we have experimentally observed Ramsey fringe with beating pattern for transmon qubits, and traced the origin to electric instruments induced flux noise. We developed a random telegraph noise (RTN) model to simulate the impact of telegraph-like flux-noise sources on Ramsey oscillations. Our simulations demonstrate that strong flux-RTN sources can induce beating patterns in the Ramsey fringes, showing excellent agreement with experimental observations in transmon qubits influenced by electronic environment-induced flux-noise. Our findings provide valuable insights into the role of flux-noise in qubit decoherence and underscore the importance of considering flux-noise RTN when analyzing nonmonotonic Ramsey fringes.

DOI: 10.1088/0256-307X/42/4/040501 CSTR: 32039.14.0256-307X.42.4.040501

1. Introduction. Ramsey oscillation is a fundamental phenomenon observed in quantum systems that allows for the investigation of qubit coherence and dynamics. The characteristics of Ramsey oscillations provide valuable insights into qubit coherence times and the interactions between qubits and their environments. For instance, the presence of strong environmental noise can cause random fluctuations in qubit transition frequencies. These fluctuations result in qubit dephasing, which manifests as an exponential decay in the Ramsey oscillations.

In addition to the monotonic decay envelope of the Ramsey oscillations, irregular Ramsey fringes have also been observed and documented in Refs. [1–8]. By analyzing deviations from ideal Ramsey oscillations, we can obtain insights into the nature and sources of noise in qubit systems, which is crucial for developing strategies to mitigate noise and enhance qubit performance. In these instances, Ramsey oscillations are often characterized by beating patterns, which are observed in Ramsey fringes are typically attributed to charge noises, such as charge drift or fluctuation, quasiparticle tunneling events through Josephson junctions, or parity switches in superconducting islands [Fig. 1(a)].[1–4,7,9] Charge fluctuation can induce a doublet line structure in the qubit transition frequency, as observed in multiple studies,[4,10–13] thereby resulting in beating patterns in Ramsey oscillations.

For superconducting qubits such as transmon qubits with large ratios of $E_{\rm j}/E_{\rm c}$ (where $E_{\rm j}$ represents the Josephson energy and $E_{\rm c}$ denotes the charging energy), flux qubits and phase qubits, charge noise is significantly mitigated. In contrast, flux noise emerges as the predominant source of noise, particularly for qubits based on SQUID structures.[11,12,14–18] Flux noise originates from fluctuations in the magnetic flux threading through SQUID structures. External magnetic field variations and the motion of magnetic vortices are known to induce flux fluctuations. Notably, the most significant flux noise is low-frequency magnetic-flux noise, characterized by a $1/f$ power density spectrum, commonly referred to as the $1/f$ flux noise.[15,19–22] Despite the proposal of several microscopic models for this $1/f$ flux noise, including random surface/interface spin reversa,[19] diffusion,[23] and clustering,[24] the exact origin of this phenomenon remains ambiguous.

Since flux noise represents one of the most significant sources of noise, it is pertinent to explore its potential role in inducing irregular Ramsey oscillations [Fig. 1(b)]. Indeed, magnetic field-dependent Ramsey beating has been sporadically observed. For example, Rower *et al.*[25] documented Ramsey beating patterns in the presence of a weak in-plane magnetic field. However, conclusive experimental evidence specifically attributing these phenomena to flux noise remains limited.

In this study, we conducted measurements on transmon qubits and observed Ramsey fringes exhibiting beating patterns. By analyzing the dependence of these beating patterns on qubit frequency, we found that they are consistent with those induced by telegraph flux noise. We traced the source of this noise to electromagnetic radiation from nearby electronic instruments and mitigated the flux

*Corresponding author. Email: leilingxiao18@nudt.edu.cn; xinfangzhang@quanta.org.cn; mtdeng@nudt.edu.cn
© 2025 Chinese Physical Society and IOP Publishing Ltd. All rights, including for text and data mining, AI training, and similar technologies, are reserved.

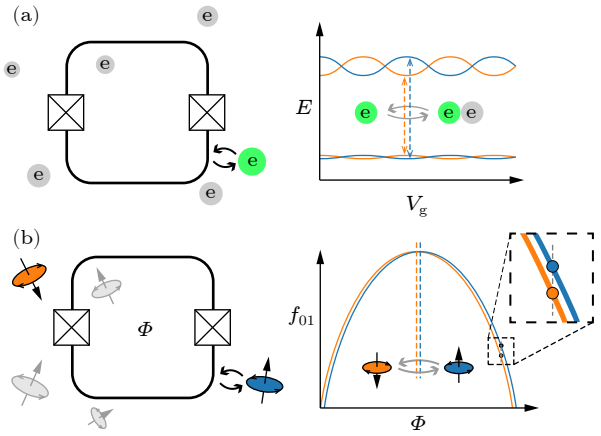

Fig. 1. Noise on superconductor quantum chip. (a) Schematic illustration of a transmon qubit coupled to charge noise sources. Charge fluctuations can induce transmon parity switches, resulting in qubit frequency splitting. (b) Schematic illustration of a transmon qubit coupled to flux noise sources. A single strongly coupled random telegraph noise (RTN) source in the flux can create a doublet structure in the qubit transition frequency, thereby causing decoherence.

noise by increasing the distance between the instruments and the dilution refrigerator. To gain deeper insights into telegraph flux noise, we developed a decoherence model for transmon qubits and integrated it with a random telegraph noise (RTN) model to simulate Ramsey oscillations. Our simulations successfully reproduced the observed beating patterns in the Ramsey fringes, demonstrating excellent agreement with experimental data.

2. Ramsey Oscillation Experiments. The transmon qubits investigated in this work are from a superconducting circuit chip featuring a structure analogous to those reported in Refs. [26,27]. On the chip, the frequency-tunable transmon qubits are interconnected by a coupling-tunable coupler qubit between adjacent transmon qubits.[28] The qubit readout is implemented by a dispersive measurement scheme with Josephson parameter amplifiers and high electron mobility transistor (HEMT) amplifiers.

We performed Ramsey measurements on the transmon qubits. Besides the monotonically decaying pattern as shown in Fig. 2(a), Ramsey oscillations with beating patterns are also observed for some qubits [Fig. 2(b)]. To further investigate the beating Ramsey envelope, we measured the frequency-dependent Ramsey oscillations for two transmon qubits, specifically qubit-1 and qubit-2. The behavior of the other three qubits, which exhibit similar characteristics, is illustrated in Fig. S2 (supplementary materials). As shown in Figs. 3(a)–3(b), the T_2^*-time of the qubits shows a significant dependence on frequency, influenced by the derivative $\mathrm{d}f_{01}/\mathrm{d}\Phi_\mathrm{b}$ [Eq. (2)]. Notably, beating patterns are evident across nearly all frequencies for both qubits, particularly for qubit-1, where the second beating node is clearly visible. The broad frequency span of the beating pattern can rule out coherently coupled two-level-system (with energy level avoided-crossing[29,30]) defects as a potential cause. The T_1 time (average for the studied frequency range) for qubit-1 and qubit-2 are 34 µs and 37 µs, respectively.

Additionally, the frequency of the beating pattern is strongly influenced by f_{01}, with faster beating observed when $\mathrm{d}f_{01}/\mathrm{d}\Phi_\mathrm{b}$ increases (i.e., when f_{01} decreases). Consequently, we hypothesize that the beating pattern originates from external flux noise. Upon a thorough examination of the measurement setup and equipment, we identified that

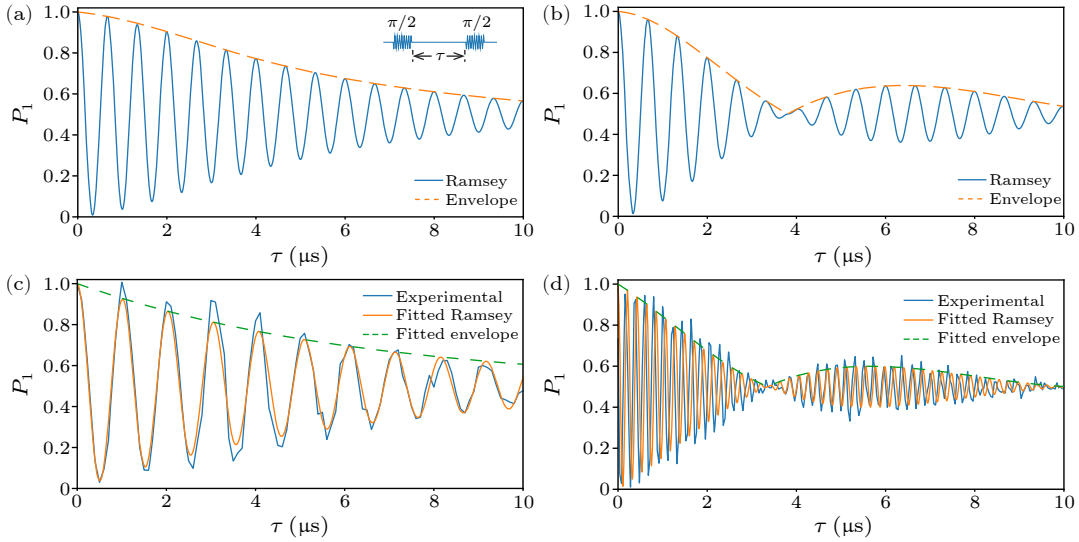

Fig. 2. Ramsey fringe of a transmon qubit. (a) Simulation result of Ramsey oscillation when only $1/f$ noise is applied to the SQUID. The inset shows the pulse sequence of a typical Ramsey experiment. (b) Simulation result of Ramsey oscillation when both $1/f$ noise and strong RTN noise are applied to the SQUID, and the beating phenomena are observed. (c) Experimental observation of Ramsey oscillations of a transmon qubit. The blue line is the measurement data, while the orange line depicts the curve fitted by the function $[1+\cos(\Delta\omega t)\exp(-\Gamma_2^* t)]/2$. The green line illustrates the fitted envelope. The Ramsey oscillation shows a monotonic decay pattern. Similar to panel (d), but showing a beating pattern in the envelope [The orange line is fitted by function in Eq. (10).].

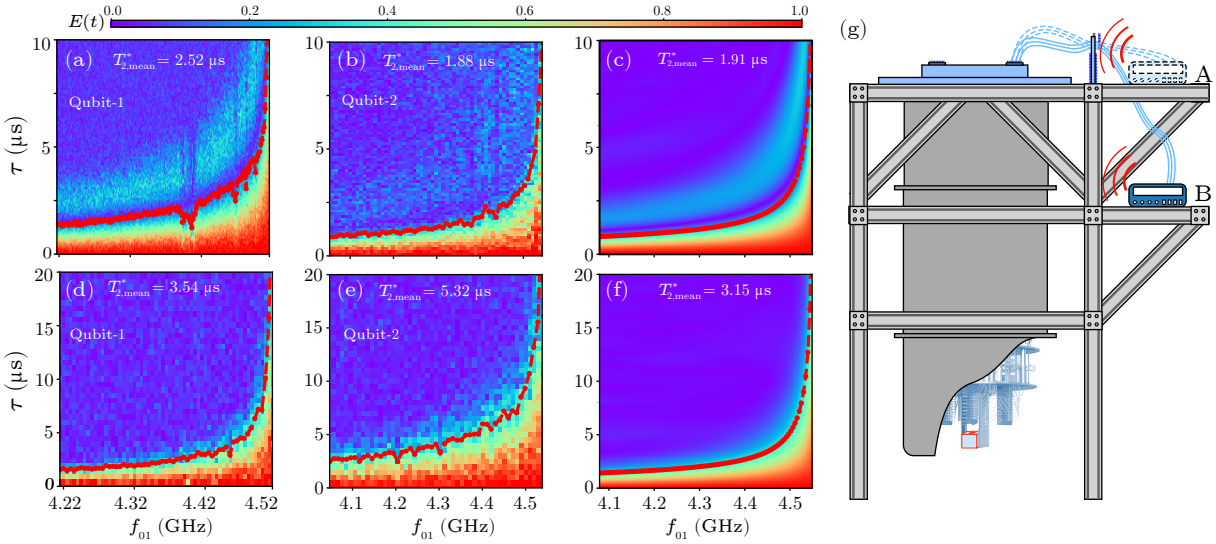

Fig. 3. Qubit-frequency dependent Ramsey fringe. (a), (b), (d) and (e) Experimental results for qubit-1 and qubit-2. The measured variable is the extracted qubit state vector XY-modulus [i.e., $E(t)$ or $E'(t)$] from the Ramsey experiment as a function of qubit frequency f_{01} and the time interval τ. Red dots represent the decoherence time T_2^* obtained by fitting the Ramsey envelopes, with the mean values of T_2^* labeled. For both qubits, the Ramsey fringe envelope exhibits exponential decay at all frequencies. T_2^* decreases significantly when the qubit is far from the optimal point. (a) and (b) exhibit a beating phenomenon across the entire tunable frequency range, while the beating pattern disappears in (d) and (e). (c) and (f) Numerical simulations with and without an additional strong RTN, respectively. The simulations are in excellent agreement with the experimental results. (g) Sketch of the measurement setup. The beating Ramsey interference pattern appears at location A and disappears at location B.

the flux noise stems from DC-source instruments used to power HEMTs. As illustrated in Figs. 3(d)–3(e), the beating patterns for both qubits vanish immediately after relocating the instruments from location A to location B [Fig. 3(g)]. We also conducted CPMG measurements [17] for the qubits (see Appendix A), which reveal significant flux noise at low frequencies.

A plausible mechanism is that the electromagnetic radiation emitted at specific frequencies by these nearby instruments induces a telegraph-like flux-noise to qubits. The quantum chip is carefully shielded by a double-layer μ-metal box. Therefore, this telegraph flux noise could be picked up by the plugboard, wires, or the fridge insert, and then transmitted via coaxial cables to the chip, thereby affecting the qubits. The impact of this radiation would be significantly reduced if the instruments were positioned farther away from the plugboard. We also noted that similar noise has also been detected by other research groups, even when using magnetic shielding (private communication with QuantumCTek and China Telecom Quantum Group).

3. Numerical Simulation. To gain deeper insights into the mechanism of telegraph flux noise, we developed a flux-RTN model and conducted numerical simulations.

3.1. Qubit Decoherence Model. We first establish a decoherence model for a transmon qubit. Considering a single transmon qubit with a symmetric SQUID structure, the qubit transition frequency $\omega_{01} \equiv 2\pi f_{01}$ can be tuned by varying the external magnetic flux Φ_b applied to the SQUID. Under the two-level approximation, the Hamiltonian of the transmon qubit is given by

$$H_\mathrm{tra} = -\frac{\hbar\omega_{01}(\Phi_\mathrm{b})}{2}\sigma_z, \tag{1}$$

where σ_z represents the Pauli-z operator. For a transmon qubit, $\omega_{01}(\Phi_\mathrm{b})$ can be approximately expressed as

$$\omega_{01}(\Phi_\mathrm{b}) = \frac{\sqrt{8E_\mathrm{c}E_\mathrm{j}|\cos(\pi\Phi_\mathrm{b}/\Phi_0)|} - E_\mathrm{c}}{\hbar}, \tag{2}$$

with $\Phi_0 \equiv \frac{\hbar}{2e}$ denoting the magnetic flux quantum.

The quantum decoherence of a transmon qubit is typically characterized by the Bloch-Redfield equation. [31,32] However, this model becomes inadequate when accounting for low-frequency noise, including $1/f$ noise. By considering all low frequency noises as an adiabatic modulation of the transmon Hamiltonian, we propose an alternative model for transmon dephasing (see Appendix D for detailed derivation). Mathematically, the decoherence can be expressed through the decay of the off-diagonal elements of the density matrix, which reads

$$\begin{aligned}\rho_{01}(t) &= \rho_{01}(0)\mathrm{e}^{-\frac{S_Q[\omega_{01}(\Phi_\mathrm{b})]}{2\hbar^2}t}\cdot\left\langle \mathrm{e}^{\mathrm{i}\int_0^t\omega'(\tau)\mathrm{d}\tau}\right\rangle_{\varepsilon\in\mathcal{E}},\\ \rho_{10}(t) &= \rho_{10}(0)\mathrm{e}^{-\frac{S_Q[\omega_{01}(\Phi_\mathrm{b})]}{2\hbar^2}t}\cdot\left\langle \mathrm{e}^{-\mathrm{i}\int_0^t\omega'(\tau)\mathrm{d}\tau}\right\rangle_{\varepsilon\in\mathcal{E}},\end{aligned} \tag{3}$$

where $\omega'(\tau) \equiv \omega_{01}[\Phi_\mathrm{b} + \delta\Phi(\tau, \varepsilon)]$, and $\delta\Phi(t, \varepsilon)$ represents a sample function of the total low-frequency noise $\delta\Phi(t)$; $\mathcal{E}$ denotes sample space encompassing all low-frequency noise components, $\langle\cdot\rangle_{\varepsilon\in\mathcal{E}} \equiv \frac{1}{|\mathcal{E}|}\sum_{\varepsilon\in\mathcal{E}}(\cdot)$. From Eq. (3), we derive the well-known relation between the relaxation time T_1 and dephasing time T_2, given by

$$T_2 = \frac{2T_1T_{2,\phi}}{2T_1 + T_{2,\phi}}, \tag{4}$$

where $T_1 = \frac{\hbar^2}{S_Q[\omega_{01}(\Phi_\mathrm{b})]}$, and $T_{2,\phi}$ represents the decay time of $|\langle \mathrm{e}^{-\mathrm{i}\int_0^t\omega'(\tau)\mathrm{d}\tau}\rangle_{\varepsilon\in\mathcal{E}}|$, assuming exponential decay.

At last, we elucidate the connection between Eq. (3) and the Ramsey experiment to facilitate subsequent discussions. In the context of the Ramsey experiment, let the detuning frequency be denoted as $\Delta\omega$. The Ramsey curve can then be expressed as

$$P_1(t) = \frac{1}{2}\left[1 + \cos(\Delta\omega t)E(t)\right], \tag{5}$$

where it is assumed that the qubit is initialized in the state $|0\rangle$. Here, $P_1(t)$ represents the population of the state $|1\rangle$ at time t, and the envelope function $E(t)$ is defined as the absolute value of the decay factor given by Eq. (3), specifically,

$$E(t) = \mathrm{e}^{-\frac{S_Q[\omega_{01}(\Phi_\mathrm{b})]}{2\hbar^2}t} \cdot \left|\langle \mathrm{e}^{\mathrm{i}\int_0^t \omega'(\tau)\mathrm{d}\tau}\rangle_{\varepsilon\in\mathcal{E}}\right|. \tag{6}$$

Here, $E(t)$ represents the evolution of the modulus of the quantum state on the Bloch XY-plane.

3.2. RTN Model. To generate the noise PSD for Eq. (6) as discussed in the previous section, it is necessary to develop a noise model capable of producing $1/f$ noise. $1/f$ noise can be understood from various perspectives. One of the most widely accepted approaches is to interpret $1/f$ noise as resulting from the superposition of a large number of bistable fluctuators.[21,33] The noise contribution from each fluctuator is characterized by random telegraph noise.[34–36]

Regarding $1/f$ flux noise, these fluctuators can be attributed to surface or interface spin random reversals or other physical phenomena discussed previously. As illustrated in Fig. 1(b), these fluctuators are distributed throughout the quantum chip hosting transmon qubits. The two stable states of a single fluctuator will induce either a positive or negative flux in the SQUID, both with equal magnitude. Given that electron spins are relatively insensitive to the surrounding environment, it is reasonable to assume that the transition rates between the two stable states of a fluctuator are identical (i.e., $\lambda_{\uparrow\to\downarrow} = \lambda_{\downarrow\to\uparrow} \equiv \lambda$). Mathematically, the flux contribution from an individual fluctuator can be expressed as an RTN, which reads

$$\mathrm{RTN}(t) = s_0 b(-1)^{N(t)}, \tag{7}$$

where s_0 is a uniform random variable with $P(s_0 = -1) = P(s_0 = +1) = 1/2$, determining the initial state of the fluctuator at $t = 0$, b represents the amplitude of the RTN, and $N(t)$ denotes a Poisson random process with a switching frequency λ.

With the RTN expressed as a stochastic process $[\mathrm{RTN}(t)]$, we can define a new stochastic process as

$$\mathrm{Flicker}(t) = \sum_{i=0}^{N} \mathrm{RTN}_i(t). \tag{8}$$

If N is sufficiently large and the switching frequency of all fluctuators $\{\lambda_i | i = 1, \cdots, N\}$ follow the distribution $P(\lambda) \propto 1/\lambda$,[21] it can be demonstrated that the PSD of $\mathrm{Flicker}(t)$ is given by (Appendix E)

$$S_{\mathrm{Flicker}}(\omega) \propto \frac{1}{\omega}, \tag{9}$$

which conforms to the definition of $1/f$ noise.

To simulate the extra telegraph flux noise (such as from the electronic instrument microwave radiation), an individual strong coupled RTN with a substantially higher amplitude can be superimposed on the $1/f$ noise spectrum. This additional noise component directly influences the f_{01} spectrum, leading to a doublet structure as illustrated in Fig. 1(b). Assuming the spectral splitting between the two stable states at the working bias Φ_b is $\delta\omega$, the modified Ramsey curve approximates to

$$P_1(t) \approx \frac{1}{2}\left[1 + \cos(\Delta\omega t)|\cos(\delta\omega t/2)|E(t)\right]. \tag{10}$$

Equation (10) implies a new Ramsey envelope $E'(t) = |\cos(\delta\omega/2t)|E(t)$, which directly indicates the Ramsey beating phenomenon.

Equation (10) could be derived strictly through the analytic discussion of decay factor $\langle \mathrm{e}^{-\mathrm{i}\int_0^t \omega'(\tau)\mathrm{d}\tau}\rangle_{\varepsilon\in\mathcal{E}}$ in Appendix C. Specifically, Eq. (S3) in the supplementary materials illustrates that the new Ramsey envelope $E'(t)$ reads

$$E'(t) = \left|\left\langle \exp\left(\mathrm{i}\int_0^t \frac{\mathrm{d}\omega_{01}}{\mathrm{d}\Phi_\mathrm{b}}\Big|_{\Phi_\mathrm{b}} \mathrm{RTN}(\tau, \varepsilon_j)\mathrm{d}\tau\right)\right\rangle_{\varepsilon\in\mathcal{E}'}\right| E(t). \tag{11}$$

Assuming the switching frequency λ is sufficiently low, the probability that the fluctuator does not switch during a single experiment, i.e. $P(n = 0)$, would be close to one. For example, if a single experiment lasts for 50 μs and $\lambda = 50\,\mathrm{Hz}$, then $P(n = 0) = 0.9975$. Regarding Eq. (S9) in the supplementary materials, the preceding discussion indicates that the expansion can be truncated to the $n = 0$ term, implying

$$E'(t) = \mathrm{e}^{-\lambda t}\left|\cos\left(\frac{\mathrm{d}\omega_{01}}{\mathrm{d}\Phi_\mathrm{b}}\Big|_{\Phi_\mathrm{b}} \cdot b \cdot t\right)\right| E(t). \tag{12}$$

Since b remains significantly smaller than Φ_0, we have $\mathrm{d}\omega_{01}/\mathrm{d}\Phi_\mathrm{b}|_{\Phi_\mathrm{b}} \cdot b \approx \delta\omega/2$. Additionally, the extra decay factor $\mathrm{e}^{-\lambda t}$ is negligible given that λ is sufficiently small. Consequently, we have derived Eq. (10).

In addition to the case caused by a single prominent RTN, we can also predict other nonmonotonic Ramsey oscillations resulting from a few prominent RTNs. Specifically, if there are N_s additional RTNs with amplitudes $\{b_j\}$, the Ramsey envelope $E''(t)$ is given by

$$E''(t) = \prod_{j=1}^{N_\mathrm{s}}\left|\cos\left(\frac{\mathrm{d}\omega_{01}}{\mathrm{d}\Phi_\mathrm{b}}\Big|_{\Phi_\mathrm{b}} \cdot b_j \cdot t\right)\right| E(t). \tag{13}$$

3.3. Simulation of Ramsey oscillation with flux-RTN. Based on the decoherence and RTN models, we can simulate the Ramsey oscillation by numerically evaluating the term $\langle \mathrm{e}^{-\mathrm{i}\int_0^t \omega'(\tau)\mathrm{d}\tau}\rangle_{\varepsilon\in\mathcal{E}}$ in Eq. (6), assuming that the PSD of quantum noise $S_\mathrm{Q}(\omega)$ remains constant across the entire tunable frequency range of the transmon qubit (details are described in Appendix B). By combining the RTN-generated PSD with the decoherence model of the transmon qubit, we can numerically simulate Ramsey oscillations. As shown in Fig. 2(a), the simulated Ramsey fringe envelope exhibits the expected exponential decay.

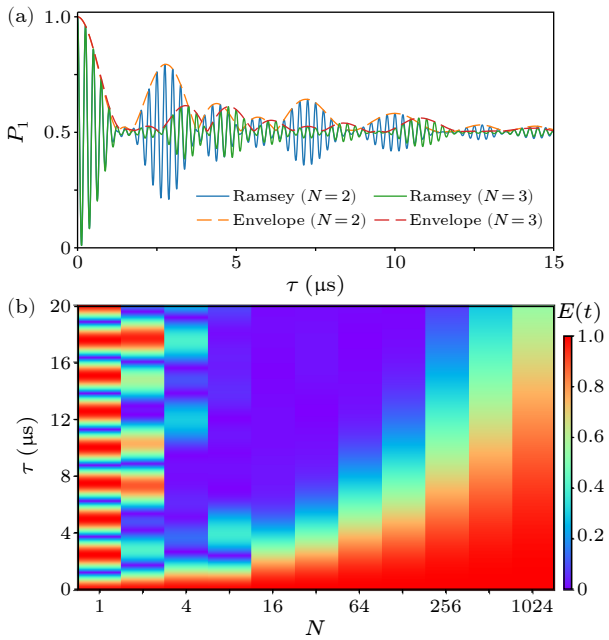

Fig. 4. Ramsey fringes induced by multiple strong flux-RTN sources. (a) Ramsey fringes in the presence of $1/f$ noise and N flux-RTN sources, where $N = 2, 3$. (b) Simulated $E(t)$ for Ramsey process as a function of N. From left to right, the amplitude of the additional flux-RTN is distributed among N individual sources. For each N, the amplitudes of individual flux-RTN sources b_i $(i = 1, 2, \ldots, N)$ are randomly generated while their total sum remains constant, i.e., $\sum_{i=1}^{N} b_i = b_0$. The spectra demonstrate how the beating pattern evolves into a typical exponential decay pattern as the influence of the additional strong flux-RTN is averaged out ($\lambda = 50\,\mathrm{Hz}$, $b_0 = 8 \times 10^{-5}\Phi_0$, $\Phi_\mathrm{b} = 0.0966\Phi_0$).

To investigate the flux-noise-induced nonmonotonic Ramsey fringe, we introduce one or a few RTN noise sources with significantly higher amplitudes into the stochastic $1/f$ process $\delta\Phi(t) = \mathrm{Flicker}(t)$. As shown by the simulated Ramsey curve in Fig. 2(b), when a strongly coupled flux-RTN is present, the Ramsey oscillation pattern exhibits a modified behavior characterized by a beating envelope. Specifically, for the strongly coupled flux-RTN, we set the switching frequency to $\lambda = 50\,\mathrm{Hz}$ and the amplitude to $b = 4.2 \times 10^{-5}\Phi_0$. Note that, according to the results shown in Fig. R7 (supplementary materials), the switching frequency does not have a significant impact on the beating phenomena, as long as it is lower than the sampling frequency. While b is directly correlated with the beating frequency $\delta\omega$ [Eq. (12)], and we set the value of b by fitting to the experimental results. For the simulated transmon qubit, we set the bias flux to $\Phi_\mathrm{b} = -0.06051\Phi_0$.

We then performed the simulation for qubit frequency dependent Ramsey oscillations in Figs. 3(c) and 3(f), with and without an additional strong flux-RTN, respectively. The simulation in Fig. 3(c) reproduces the f_{01}-dependent beating pattern. The excellent agreement between simulation and the measurement confirms that the observed beating pattern of Ramsey can be attributed to one or a few telegraph-like flux-noise sources that are strongly coupled to the qubits (which is the electric instrument microwave radiation in this case).

If multiple strong RTNs with varying amplitudes are present, the Ramsey fringe envelope becomes increasingly irregular. As illustrated in Fig. 4(a), Ramsey fringes with $N = 2$ and $N = 3$ strong RTNs exhibit complex beating patterns, and the damping of Ramsey oscillations increases as N grows. In fact, when noise sources transition from a "strong-but-few" scenario to a "weak-but-many" scenario, the Ramsey fringe pattern evolves from a beating pattern to an exponentially decaying one [Fig. 4(b)].

4. Conclusion. In this paper, we have observed beating Ramsey fringes in frequency-tunable transmon qubits. The beating pattern is found to be dependent on the qubit frequency and influenced by the positioning of an electronic instrument. We attribute the non-monotonic Ramsey pattern to electromagnetic radiation noise originating from the instrument. To model this phenomenon, we developed a flux-RTN model and simulated the beating Ramsey fringes, achieving excellent agreement with the experimental data. Our results demonstrate that telegraph-like flux noise can induce a beating Ramsey pattern similar to charge noise and indicate that it is important to minimize possible electromagnetic noise from electric instruments. Also, although the flux noise in this experiment originates from a macroscopic environment, our findings can be extended to microscopic flux noise, which provides insights into analyzing qubit decoherence channels[37,38] through Ramsey experiments.

Acknowledgements. We would like to express our gratitude to Yang Yang, Xiao-Feng Yi, Yi-Chuan Zeng, and Wei-Chen Wang for their technical assistance with qubit measurements. We also thank Shao-Jun Guo and Wen-Hao Chu for insightful discussions. This work was supported by the National Key Research and Development Program of China (Grant No. 2024YFB4504001). We also thank Tianyan Quantum Computing Cloud Platform for supporting.

References

[1] Ristè D, Bultink C C, Tiggelman M J, Schouten R N *et al.* 2013 *Nature Communications* **4** 1913
[2] Stern M, Catelani G, Kubo Y *et al.* 2014 *Physical Review Letters* **113** 123601
[3] Peterer M J, Bader S J, Jin X *et al.* 2015 *Physical Review Letters* **114** 010501
[4] Luthi F, Stavenga T, Enzing O W *et al.* 2018 *Physical Review Letters* **120** 100502
[5] von Lüpke U, Beaudoin F, Norris L M *et al.* 2020 *PRX Quantum* **1** 010305
[6] Ni Z, Li S, Zhang L *et al.* 2022 *Physical Review Letters* **129** 040502
[7] Martinez L A, Peng Z, Appelö D *et al.* 2023 *Applied Physics Letters* **22** 1
[8] Evert B, Izquierdo Z G, Sud J *et al.* 2024 arXiv:2403.07836 [quant-ph]
[9] Chang T, Holzman I, Cohen T *et al.* 2022 *Physical Review Applied* **18** 064062
[10] Bertet P, Chiorescu I, Burkard G *et al.* 2005 *Physical Review Letters* **95** 257002
[11] Yoshihara F, Harrabi K, Niskanen A O *et al.* 2006 *Physical Review Letters* **97** 167001

[12] Schreier J A, Houck A A, Koch J *et al.* 2008 *Physical Review B* **77** 180502
[13] Bal M, Ansari M H, Orgiazzi J L *et al.* 2015 *Physical Review B* **91** 195434
[14] Koch J, Yu T M, Gambetta J *et al.* 2007 *Physical Review A* **76** 042319
[15] Bialczak R C, McDermott R, Ansmann M *et al.* 2007 *Physical Review Letters* **99** 187006
[16] Kakuyanagi K, Meno T, Saito S *et al.* 2007 *Physical Review Letters* **98** 047004
[17] Bylander J, Gustavsson S, Yan F *et al.* 2011 *Nature Physics* **7** 565
[18] Sank D, Barends R, Bialczak R C *et al.* 2012 *Physical Review Letters* **109** 067001
[19] Koch R H, DiVincenzo D P, and Clarke J 2007 *Physical Review Letters* **98** 267003
[20] Zhou D and Joynt R 2012 *Superconductor Science and Technology* **25** 045003
[21] Paladino E, Galperin Y M, Falci G *et al.* 2014 *Reviews of Modern Physics* **86** 361
[22] Falci G, Hakonen P J, and Paladino E 2024 *Encyclopedia of Condensed Matter Physics* (Leiden, Netherlands: Elsevier)
[23] Lanting T, Amin M H, and Berkley A J 2014 *Physical Review B* **89** 014503
[24] De A 2014 *Physical Review Letters* **113** 217002
[25] Rower D A, Ateshian L, Li, L H *et al.* 2023 *Physical Review Letters* **130** 220602
[26] Arute F, Arya K, Babbush R *et al.* 2019 *Nature* **574** 505
[27] Wu Y, Bao W S, Cao S *et al.* 2021 *Physical Review Letters* **127** 180501
[28] Yan F, Krantz P, Sung Y *et al.* 2018 *Physical Review Applied* **10** 054062
[29] Martinis J M, Cooper K B, McDermott R *et al.* 2005 *Physical Review Letters* **95** 210503
[30] Müller C, Cole J H, and Lisenfeld J 2019 *Reports on Progress in Physics* **82** 124501
[31] Bloch F 1957 *Physical Review* **105** 1206
[32] Redfield A G 1957 *IBM Journal of Research and Development* **1** 19
[33] Kogan S and Nagaev K 1984 *Solid State Communications* **49** 387
[34] Machlup S 1954 *Journal of Applied Physics* **25** 341
[35] Kirton M J and Uren M J 1989 *Advances in Physics* **38** 367
[36] Kogan S 1996 *Electronic Noise and Fluctuations in Solids* (Cambridge, UK: Cambridge University Press)
[37] Braumüller J, Ding L, Vepsäläinen A P *et al.* 2020 *Physical Review Applied* **13** 054079
[38] Zhang X F, Wu Z H, White G A L *et al.* 2025 *Communications Physics* **8** 29